Ab Initio Direct Dynamics Trajectory Study of the $Cl^- + CH_3Cl$ S_N2 Reaction at High Reagent Translational Energy

Guosheng Li and William L. Hase*

Contribution from the Department of Chemistry, Wayne State University, Detroit, Michigan 48202

Received February 25, 1999

Abstract: An ab initio (HF/3-21+G*) direct dynamics quasiclassical trajectory study was performed for the $Cl^- + CH_3Cl$ S_N2 reaction at a reagent relative translational energy of 100 kcal/mol. Initial conditions for the trajectories were averaged over the orientation of CH_3Cl and the reaction dynamics studied versus collision impact parameter. The trajectories reacted by a backside attack mechanism and reaction by frontside attack was not observed. The calculated backside reaction cross reaction is 0.22−0.40 Å^2 and approximately two to four times larger than the experimental value (*J. Phys. Chem. A* **1997**, *101*, 5969). The absence of reaction by frontside attack was investigated by initiating trajectories at the C_s transition state for the frontside attack mechanism. These trajectories formed $Cl^- + CH_3Cl$ reactants with a large vibrational energy and low relative translational energy, which suggests extensive CH_3Cl vibrational excitation is needed to access the frontside reaction pathway.

I. Introduction

The dynamics, kinetics, and energetics of the thermoneutral symmetric nucleophilic substitution reaction

$$Cl^- + CH_3Cl \rightarrow ClCH_3 + Cl^- \qquad (1)$$

has been widely studied both experimentally[1−4] and theoretically.[5−25] A particularly interesting aspect of this reaction is its mechanism.[26−30] The original mechanism proposed by Brauman and co-workers,[27,31] for thermal conditions, is indirect backside attack in which a $Cl^-\cdots CH_3Cl$ ion−dipole complex is formed prior to surmounting the central barrier and forming products. Both classical trajectory[6,12,17,28,29] and quantum dynamical[22,25] calculations have suggested that, for collisions with a thermal reactant translational energy, C−Cl stretch excitation, and low CH_3Cl rotational energy, the S_N2 reaction may also occur by a direct backside mechanism without forming the ion−dipole complex. Since this mechanism is suppressed by CH_3Cl rotational energy and the population of excited C−Cl stretch vibrational states is small at 300 K,[17,28] it may only become a significant component to the overall reaction for high-temperature and/or nonthermal conditions.

Both experiments and theories have probed the mechanism for reaction 1 at high energies. In pioneering work by Bierbaum and co-workers,[1] the rate constant for reaction 1 was measured as a function of center-of-mass collision energy E_{rel} (i.e. translational activation) for a CH_3Cl temperature of 300 K. Deconvolution of these experiments yielded an apparent threshold of 45 kcal/mol, which was attributed to a high-energy mechanism involving frontside anionic attack at the chlorine atom of chloromethane. Such a threshold is consistent with ab initio calculations[18,21] of the barrier for a frontside mechanism in which Cl^- attacks carbon instead of chlorine. In recent experiments,[4] the translational activation of reaction 1 was studied with finer resolution of the collision energy. A translational threshold of 11 ± 4 kcal/mol was found for reaction, presumably by backside attack. No evidence for a frontside

(1) Barlow, S. E.; Van Doren, J. M.; Bierbaum, V. M. *J. Am. Chem. Soc.* **1988**, *110*, 7240.
(2) Van Doren, J. M.; DePuy, C. H.; Bierbaum, V. M. *J. Phys. Chem.* **1989**, *93*, 1130.
(3) Li, C.; Ross, P.; Szulejko, J. E.; McMahon, T. B. *J. Am. Chem. Soc.* **1996**, *118*, 9360.
(4) DeTuri, V. F.; Hintz, P. A.; Ervin, K. M. *J. Phys. Chem. A* **1997**, *101*, 5969.
(5) Shi, Z.; Boyd, R. J. *J. Am. Chem. Soc.* **1989**, *111*, 1575.
(6) Vande Linde, S. R.; Hase, W. L. *J. Am. Chem. Soc.* **1989**, *111*, 2349.
(7) Tucker, S. C.; Truhlar, D. G. *J. Phys. Chem.* **1989**, *93*, 8138.
(8) Tucker, S. C.; Truhlar, D. G. *J. Am. Chem. Soc.* **1990**, *112*, 3338.
(9) Vetter, R.; Zülicke, L. *J. Am. Chem. Soc.* **1990**, *112*, 5136.
(10) Vande Linde, S. R.; Hase, W. L. *J. Phys. Chem.* **1990**, *94*, 2778.
(11) Vande Linde, S. R.; Hase, W. L. *J. Phys. Chem.* **1990**, *94*, 6148.
(12) Vande Linde, S. R.; Hase, W. L. *J. Chem. Phys.* **1990**, *93*, 7962.
(13) Zhao, X. G.; Tucker, S. C.; Truhlar, D. G. *J. Am. Chem. Soc.* **1991**, *113*, 826.
(14) Cho, Y. J.; Vande Linde, S. R.; Zhu, L.; Hase, W. L. *J. Chem. Phys.* **1992**, *96*, 8275.
(15) Jensen, F. *Chem. Phys. Lett.* **1992**, *196*, 368.
(16) Billing, G. D. *Chem. Phys.* **1992**, *159*, 109.
(17) Hase, W. L.; Cho, Y. J. *J. Chem. Phys.* **1993**, *98*, 8626.
(18) Deng, L.; Branchadell, V.; Ziegler, T. *J. Am. Chem. Soc.* **1994**, *116*, 10645.
(19) Peslherbe, G. H.; Wang, H.; Hase, W. L. *J. Chem. Phys.* **1995**, *102*, 5626.
(20) Glukhovtsev, M. N.; Pross, A.; Radom, L. *J. Am. Chem. Soc.* **1995**, *117*, 2024.
(21) Glukhovtsev, M. N.; Pross, A.; Schlegel, H. B.; Bach, R. D.; Radom, L. *J. Am. Chem. Soc.* **1996**, *118*, 11258.
(22) Clary, D. C.; Palma, J. *J. Chem. Phys.* **1997**, *106*, 575.
(23) Mann, D. J.; Hase, W. L. *J. Phys. Chem. A* **1998**, *102*, 6208.
(24) Botschwina, P. *Theor. Chem. Acc.* **1998**, *99*, 426.
(25) Schmatz, S.; Clary, D. C. *J. Chem. Phys.* **1998**, *109*, 8200.
(26) Shaik, S. S.; Schlegel, H. B.; Wolfe, S. *Theoretical Aspects of Physical Organic Chemistry: The S_N2 Mechanism*; John Wiley and Sons: New York, 1992.
(27) Moylan, C. R.; Brauman, J. I. In *Advances in Classical Trajectory Methods: Dynamics of Ion−Molecule Complexes*; Hase, W. L., Ed.; JAI Press: Greenwich, CT, 1994; Vol. 2, p 95.
(28) Hase, W. L. *Science* **1994**, *266*, 998.
(29) Hase, W. L.; Wang, H.; Peslherbe, G. H. In *Advances in Gas-Phase Ion Chemistry*; Adams, N. G., Babcock, L. M., Eds.; JAI Press: Greenwich, CT, 1998; Vol. 3, p 125.
(30) Chabinyc, M. L.; Craig, S. L.; Regan, C. K.; Brauman, J. I. *Science* **1998**, *279*, 1882.
(31) Olmstead, W. N.; Brauman, J. I. *J. Am. Chem. Soc.* **1977**, *99*, 4219.

10.1021/ja990607j CCC: $18.00
Published on Web 07/16/1999

attack mechanism was seen in measurements of the rate constant versus translational energy,[4] and the origin of the difference with the earlier experimental study[1] is unclear. This translational threshold of 11 ± 4 kcal/mol is appreciably larger than the backside potential energy barrier of 2.5−3.0 kcal/mol, determined from ab initio calculations[24,32] and fits of statistical theories[32] to the 300 K thermal rate constant.[2] However, a translational threshold larger than the backside barrier is consistent with trajectory calculations,[6,12,17] which indicate reaction is promoted by C−Cl stretch excitation.

The translational activation of reaction 1 was recently investigated by classical trajectory simulations.[23] The shape of the experimental reaction cross section versus E_{rel} was reproduced by the trajectories and the resulting threshold of 18 kcal/mol was in approximate agreement with the experimental value. The reactive trajectories were direct, with negligible trapping in the ion−dipole complexes. The product energy was primarily partitioned to relative translation with small and similar amounts of energy partitioned to vibration and rotation. Backward scattering and a rebound mechanism was found at low E_{rel}, with increasing importance of forward scattering and a stripping mechanism as E_{rel} is increased. The total angular momentum is well-approximated by the initial orbital angular momentum, which is strongly correlated with the final orbital angular momentum. The principal difference between the trajectories and experiments is the order of magnitude larger cross sections found from the trajectories. The analytic potential energy surface (PES) used in the trajectory study did not include a mechanism (or mechanisms) for frontside attack[33] and, therefore, the trajectories were unable to predict information about the relative importance of backside versus frontside attack at high E_{rel}.

In the work reported here, the ab initio direct dynamics quasiclassical trajectory method[34−36] is used in an attempt to resolve some of the issues regarding the dynamics of reaction 1 at high E_{rel}. Of particular interest is (1) the contribution of the frontside attack pathway to the reaction rate, (2) the origin of the order of magnitude difference between the experimental and trajectory reaction cross sections versus E_{rel}, and (3) the comparison with the high E_{rel} reaction dynamics predicted by the previous trajectory study.[23]

II. Computational Procedure

A. Ab Initio Theory. Ab initio direct dynamics simulations are very computationally intensive[36] and a balance between level of ab initio theory and number of integration steps per trajectory is required. For the work reported here, calculations at E_{rel} of 100 kcal/mol and at the HF/3-21+G* level of theory were feasible and realistic. At this high E_{rel} all the trajectories are direct and each reactive event required approximately 500 integration steps (see discussion below). The HF/3-21+G* level of theory is tractable for the direct dynamics and gives stationary point properties in good agreement with those obtained from much higher levels of theory. For the backside D_{3h} barrier, the HF/3-21+G*, G2(+),[20] and CCSD(T)[24] calculations give respectively 1.8, 2.3, and 2.7 kcal/mol (zero-point energy included) for the potential energy and 2.397, 2.317, and 2.301 Å for the C−Cl bond length. A similar relationship between HF/3-21+G* and higher levels of theory is found for properties of the frontside C_s barrier, with the structures:

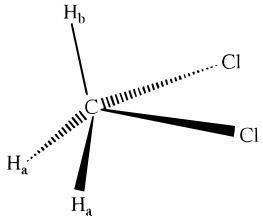

C_s

HF/3-21+G*, MP2/6-311++G**,[18] and G2(+)[21] calculations give respectively 52.9, 55.3, and 46.3 kcal/mol for the barrier's potential energy (zero-point energy included). HF/3-21+G* and MP2/6-31+G*[21] give respectively a C−Cl bond length of 2.705 and 2.438 Å and a Cl−C−Cl angle of 92.8 and 84.2° at the barrier. The HF/3-21+G* harmonic frequencies at the potential barriers are in excellent agreement with those found from higher levels of theory. HF/3-21+G* and MP2/6-31G** frequencies[7,8,18] differ on average by only 7.1 and 3.1% at the backside D_{3h} and frontside C_s transition states, respectively.

Direct dynamics trajectories were also initiated at the C_s barrier to determine the nature of the product energy partitioning for trajectories that reach this region of the potential surface. HF/3-21+G* and MP2/6-31G* trajectories were calculated and compared for this study.

B. Integrating the Quasiclassical Trajectories. The trajectory study was performed using the general chemical dynamics program VENUS96[37] interfaced with the Gaussian 98 packages of program.[38] VENUS called Gaussian to obtain the gradient of the potential for integrating the classical equations of motions.[39] Standard algorithms[40] in VENUS96 were used for selecting the trajectory initial conditions, performing the numerical integration, and analyzing the trajectory results. Each trajectory was integrated with a 0.5 fs time step for a maximum of approximately 500 integration steps. The trajectory events were direct,lasting only 250 fs or less. Integrating one trajectory for 500 steps required about 18 h on one processor of a CRAY J-916 and 7 h on one processor of a SGI/MIPS R10000 computer.

To simulate reaction 1, the reactants must have an initial separation large enough that the results are not affected by the value of the separation. Because of the high E_{rel} of 100 kcal/mol and the 300 K rotational energy for CH_3Cl considered in this study, it is possible to initially separate Cl^- from the CH_3Cl center of mass by only 10 Å. With the high reagent relative velocity and the CH_3Cl angular momentum, the initial random orientation of CH_3Cl is unaffected as the Cl^- and CH_3Cl separation moves inward to 10 Å.[41] The quasiclassical method[40] was used to add zero-point energy (zpe) to each CH_3Cl normal mode[42] and $RT/2$ rotational energy ($T = 300$ K) was added to

(32) See discussions in ref 4.

(33) It is a particularly difficult task to construct an analytic PES for reaction 1 that includes both backside and frontside reaction mechanisms.

(34) Helgaker, T.; Uggerud, E.; Jensen, H. *Chem. Phys. Lett.* **1990**, 173, *145*. Uggerud, E.; Helgaker, T. *J. Am. Chem. Soc.* **1992**, *114*, 4266.

(35) Chen, W.; Hase, W. L.; Schlegel, H. B. *Chem. Phys. Lett.* **1994**, *228*, 436.

(36) Bolton, K.; Hase, W. L.; Peslherbe, G. H. In *Modern Methods for Multidimensional Dynamics Computations in Chemistry*; Thompson, D. L., Ed.; World Scientific: River Edge, NJ, 1998; pp 143−189.

(37) Hase, W. L.; Duchovic, R. J.; Hu, X.; Komornicki, A.; Lim, K. F.; Lu, D.-H.; Peslherbe, G. H.; Swamy, K. N.; Vande Linde, S. R.; Varandas, A.; Wang, H.; Wolf, R. J. *QCPE* **1996**, *16*, 671.

(38) Frisch, M. J.; Trucks, G. W.; Schlegel, H. B.; Scuseria, G. E.; Robb, M. A.; Cheeseman, J. R.; Zakrzewski, V. G.; Montgomery, J. A., Jr.; Stratmann, R. E.; Burant, J. C.; Dapprich, S.; Millam, J. M.; Daniels, A. D.; Kudin, K. N.; Strain, M. C.; Farkas, O.; Tomasi, J.; Barone, V.; Cossi, M.; Cammi, R.; Mennucci, B.; Pomelli, C.; Adamo, C.; Clifford, S.; Ochterski, J.; Petersson, G. A.; Ayala, P. Y.; Cui, Q.; Morokuma, K.; Malick, D. K.; Rabuck, A. D.; Raghavachari, K.; Foresman, J. B.; Cioslowski, J.; Ortiz, J. V.; Stefanov, B. B.; Liu, G.; Liashenko, A.; Piskorz, P.; Komaromi, I.; Gomperts, R.; Martin, R. L.; Fox, D. J.; Keith, T.; Al-Laham, M. A.; Peng, C. Y.; Nanayakkara, A.; Gonzalez, C.; Challacombe, M.; Gill, P. M. W.; Johnson, B.; Chen, W.; Wong, M. W.; Andres, J. L.; Gonzalez, C.; Head-Gordon, M.; Replogle, E. S.; Pople, J. A. *Gaussian 98*; Gaussian, Inc.: Pittsburgh, PA, 1998.

(39) For zero total angular momentum an algorithm based on a local quadratic expansion of the potential may be used to integrate the trajectories[35] and, therefore, an ab initio calculation is not necessory at each integration step. This approach becomes less efficient if the total angular momentum is not zero (i.e.: Bolton, K.; Schlegel, H. B.; Hase, W. L.; Song, K. *Phys. Chem. Chem. Phys.*, **1999**, *1*, 999) and an ab initio calculation was performed at each integration step for the trajectories reported here.

(40) Chapman, S.; Bunker, D. L. *J. Chem. Phys.* **1975**, *62*, 2890. Sloane, C. S.; Hase, W. L. *J. Chem. Phys.* **1977**, *66*, 1523. Hase, W. L.; Ludlow, D. M.; Wolf, R. J.; Schlick, T. *J. Phys. Chem.* **1981**, *85*, 958.

(41) For 300 K reactant rotational and translational energies, the $Cl^- + CH_3Cl$ separation has been set at 30 Å in previous work.[17] A much larger separation is required if the CH_3Cl rotational energy is zero.

Table 1. Average and Range of Values for Dynamical Properties of the Reactive Trajectories[a]

property	collision impact parameter		
	$b = 0$	$b = 1$	$b = 2$
Cl−C−Cl angle[b]			
reactant	149 (130−168)	144 (127−163)	121
transition state	161 (151−170)	155 (139−170)	170
energy partitioning[c]			
f_{rel}	0.89 (0.73−0.97)	0.88 (0.62−0.95)	0.68
f_{vib}	0.10 (0.00−0.26)	0.07 (0.00−0.29)	0.11
f_{rot}	0.01 (0.00−0.04)	0.05 (0.02−0.09)	0.21
angular momenta[d]			
J	22.4	218.8 (208.8−229.9)	405.2
l_f	38.8 (16.1−66.9)	179.3 (138.1−207.7)	287.2
j_f	22.8 (7.2−47.3)	51.2 (28.4−71.7)	121.4
scattering angles[e]			
$\theta(v_i,v_f)$	173 (168−178)	141 (132−150)	108
$\theta(l_i,l_f)$		10 (5−16)	7
$\theta(l_f,J)$	25 (11−79)	7 (3−16)	5
$\theta(l_i,j_f)$		29 (6−71)	10
$\theta(l_f,j_f)$	37, 153 (37,126−168)[f]	38 (12−84)	16

[a] The range of values is given in parentheses. The reactant's impact parameter is in Å. [b] The Cl−C−Cl angle is in deg. [c] Fraction of the available energy (not including CH_3Cl zero-point energy) partitioned to product relative to translational, vibrational, and rotational energy. [d] The initial orbital angular momentum l_i is 207.9$\hbar$ and 415.7$\hbar$ for $b = 1$ and 2 Å calculations, respectively. The initial CH_3Cl rotational angular momentum j_i is 22.4$\hbar$ for each calculation. [e] Scattering angles in deg between the initial (i) and final (f), relative velocity (v), orbital angular momentum (l), CH_3Cl rotational angular momentum (j), and total angular momentum (J). [f] A bimodal $\theta(l_f,j_f)$ distribution is observed for $b = 0$ (see text). One reactive trajectory has a small $\theta(l_f,j_f)$ angle of 37°, while the average of the remaining seven is 153° and much larger.

each CH_3Cl principal rotation axis. These energies were then transformed to the Cartesian coordinates and momenta used in the numerical integrations by choosing random phase for the normal modes of vibration and random signs for the components of the angular momentum. CH_3Cl was then randomly rotated and the $Cl^- + CH_3Cl$ center-of-mass separation set at 10 Å, with an initial relative velocity for $E_{rel} = 100$ kcal/mol and the specified collision impact parameter b. The total classical energy (i.e. CH_3Cl zpe and rotation, and E_{rel}) for these initial conditions is then $25.5 + 0.9 + 100.0 = 126.4$ kcal/mol. However, at the initial $Cl^- + CH_3Cl$ separation of 10 Å there is a relatively small intermolecular interaction between reactants, which ranges from −1.8 to 1.4 kcal/mol for Cl−C−Cl angles of 180 and 0°, respectively. This adds a small breadth to the reactants' initial energy.

III. Trajectory Results and Discussions

A. Reaction Mechanism and Dynamics for Backside Attack. Due to the computational expense of this study, an attempt was made to reduce the number of nonreactive trajectories, while still calculating reaction probabilities. This was done by scanning the Cl−C−Cl angle θ of the randomly chosen initial conditions. The structures for the backside D_{3h} and frontside C_s barriers suggest the preferential Cl−C−Cl angles for reaction should be 180 and 90°, respectively, and the backside pathway was studied quantitatively and the frontside pathway qualitatively by only running trajectories with an initial θ angle in the range of 180−90°. The reaction dynamics was investigated in this manner for collision impact parameters of 0, 1, and 2 Å. For each of these impact parameters, 200 initial conditions were randomly selected and those with a θ angle of 90° or more were propagated until either products or reactants were separated by 10 Å. There were eight, seven, and one reactive trajectories for b of 0, 1, and 2, respectively, all occurring by the backside displacement mechanism. No reaction was observed for θ less than 120°. For the randomly chosen initial conditions, with b of 0 and 1 Å, the ratio of reaction to total number of trajectories is 0/34, 0/32, 0/29, 2/27, 3/24, 4/18, 2/5, and 4/11 for the initial θ angle in the range of 90−100, 100−110, 110−120, 120−130, 130−140, 140−150, 150−160, and 160−170, respectively.[43] The reaction probability is approximately 40% for θ near 180°, but negligibly small for θ close to 90°.[44]

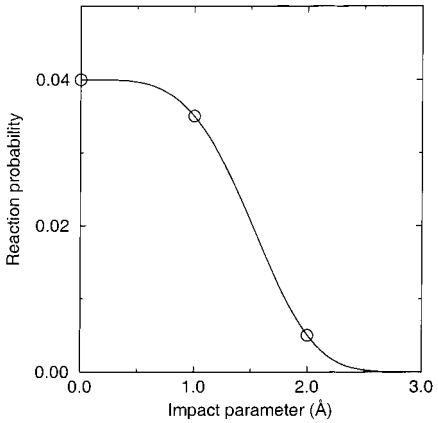

Figure 1. Probability of reaction versus impact parameter. The fit (solid line) is described in the text.

From the above number of reactive trajectories, the resulting reaction probabilities for backside displacement are 0.04, 0.035, and 0.005 for b of 0, 1, and 2 Å, respectively. They are plotted in Figure 1, where they are fit with the function $P_r(b) = 0.04 \exp(-0.134b^{3.96})$. This expression for $P_r(b)$ may be inserted into

$$\sigma = \int_0^\infty P_r(b) 2\pi b \, db \qquad (2)$$

to estimate the reaction cross section. The resulting value is 0.31 Å^2. Computing the standard deviation in the reaction probability at each b, from the square root of the number of reactive events, gives a reaction cross section in the range of 0.22−0.40 Å^2, which is approximately two to four times larger than the experimental value of 0.11 Å^2 for $E_{rel} = 100$ kcal/mol.[4]

(42) At 300 K there is negligible excitation of the CH_3Cl vibrational modes.

(43) The probability of an initial Cl−C−Cl angle θ is proportional to $\sin\theta$ and none of the 200 initial conditions for each b had a value for θ in the range of 170−180°.

(44) Twenty trajectories were run with $b = 0$ and random values of θ between 0 and 90°. No reaction by either backside or frontside attack was found.

The trajectory cross section, based on the analytic potential energy surface PES3, is 3.05 Å^2 for $E_{rel} = 100$ kcal/mol and the same type of CH_3Cl energies as used for the above direct dynamics.[45] The value of b_{max} for this calculation is 3.0 Å and similar to the value estimated from Figure 1, which indicates that the difference between the reactive cross sections for the current and previous trajectory studies arises not from different b_{max} values but from a near order of magnitude difference in reaction probabilities.

Properties of the direct dynamics reactive trajectories are summarized in Table 1. In crossing the transition state (defined by equal C−Cl bond lengths) the Cl−C−Cl angle tends to increase, coming close to the backside reaction path value of 180°. The product energy is primarily partitioned to relative translation, with much smaller amounts to CH_3Cl vibration and rotation. Energy partitioning to product rotation increases with increase in impact parameter. The velocity scattering angle shows strong backward scattering and a rebound mechanism for $b = 0$, but a tendency toward forward scattering and a possible stripping mechanism (see Figure 5 in ref 23) as b is increased. A higher rotational energy as b is increased is consistent with a stripping mechanism.[23]

The angular momentum scattering angles for $b = 1$ and 2 Å provide a rather detailed picture of the atomic motion during the reaction. The near alignment of the initial and final orbital angular momenta, l_i and l_f, means that the motion of Cl^- and the center of mass of CH_3Cl is approximately in the same plane for both reactants and products. Since the initial CH_3Cl rotational angular momentum j_i is small compared to l_i, the total angular J and l_i are nearly equal and, thus, J and l_f are aligned. The orbital angular momentum of the products l_f is smaller than that of the reactants l_i, and for the total angular momentum to be conserved, i.e., $l_i \approx J = l_f + j_f$, l_f and j_f must point in the same direction. Thus, the angular velocities for the product CH_3Cl and orbital rotations are in the same direction.

For $b = 0$ trajectories the $\theta(l_f,j_f)$ scattering angles are considerably different from those for the larger impact parameters. This arises from the small total angular momentum for $b = 0$. If j_i was zero for $b = 0$, $\theta(l_f,j_f)$ would have to equal 180° to conserve the total angular momentum of zero. For the trajectories reported here with a small j_i of 22.4$\hbar$, seven of the reactive events qualitatively retain this relation between l_f and j_f. However, one of the reactions has small $l_f = 16.1\hbar$ and $j_f = 7.2\hbar$, which are approximately aligned with $\theta(l_f,j_f) = 37°$.

The energy partitioning, velocity scattering angle distribution, and angular momentum correlations for these direct dynamics trajectories and the trajectories studied previously,[23] for the PES3 analytical potential, are very similar. However, as noted above the PES3 reaction cross section is an order of magnitude larger than the HF/3-21+G* direct dynamics value. Since trajectory calculations with analytical potentials are much faster than ab initio direct dynamics, it is of interest to determine what regions of the PES3 surface are in error. A previous comparison of PES3 and MP2/6-311+G** surfaces,[23] in the vicinity of the central barrier, showed that the PES3 energies are somewhat lower, which would result in more reaction on PES3. More complete comparisons between PES3 and ab initio calculations in the region between the pre- and postreaction $Cl^-\cdots CH_3Cl$ complexes show that the PES3 energies are particularly too low for distortions of the CH_3 umbrella. Extensive ab initio calculations at both low and high energies will be needed to correct PES3.

(45) For a 300 K Boltzmann distribution of CH_3Cl vibrational and rotational energies, the cross section is 3.54 Å^2 and $b_{max} = 2.7$ Å. Mann, D. J.; Hase, W. L. Unpublished results.

B. Search for Frontside Reaction. As discussed above, though the initial conditions chosen for the trajectories are those expected to facilitate frontside attack, reaction by frontside attack was not observed in the direct dynamics trajectories. The small impact parameters for the initial conditions have a small centrifugal potential and, thus, more vibrational kinetic energy available to deform the $Cl^- + CH_3Cl$ system to attain the C_s barrier region of the potential energy surface. In addition, ab initio calculations[18,21] show that the frontside reaction pathway is initially Cl^- approaching backside and then moving frontside for displacement with retention of configuration. Thus, initial Cl−C−Cl angles between 180 and 90° are expected to be favorable for frontside reaction.

It is of interest that one of the $b = 1$ Å nonreactive trajectories attained the approximate C_{2v} configuration

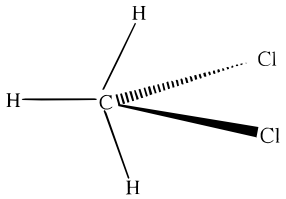

C_{2V}

with equal C−Cl bond lengths of 2.9 Å and a Cl−C−Cl angle of 102.1°. Except for the orientation of the CH_3 group, this C_{2v} configuration has a structure quite similar to that of the frontside C_s barrier. All that is required for a transition from the C_{2v} to C_s configuration is an approximate 90° rotation of the methyl group. At the HF/3-21+G* level this barrier is relatively small, ~10 kcal/mol, suggesting such a rotation is possible to give reaction through the frontside mechanism. In an attempt to induce this mechanism, 200 trajectories were run as above with $b = 1$ Å and an initial Cl−C−Cl angle between 180 and 90°, but with an additional 4 quanta of energy added to each of the two symmetric rocking modes of CH_3Cl. The frequency for these modes is 1142 cm^{-1}, and these 8 additional quanta add 26.1 kcal/mol of vibrational energy to CH_3Cl, possibly assisting CH_3 rotation and promoting frontside reaction. The result was negative. Only four reactive trajectories were observed, fewer than the seven reactive events without this CH_3 rocking excitation, and all occurred by backside attack.[46]

A clue to why frontside reaction is not observed in the trajectories was found by determining the energies of the products for the nonreactive trajectory which attained the approximate C_{2v} configuration. With CH_3Cl zero-point energy removed, the fractions partitioned to relative translation, vibration, and rotation are 0.20, 0.74, and 0.06, respectively. Comparing these fractions with those in Table 1, for backside reaction, shows that the sizes of the f_{rel} and f_{vib} values are reversed for the C_{2v} configuration. The implication is that to reach a configuration, like that of the frontside C_s barrier, substantial CH_3Cl reactant vibrational excitation is required.

To study, in more detail, the reactant energies needed for frontside reaction, a set of 24 trajectories were initiated at the frontside C_s barrier with a total classical energy identical with that for the $Cl^- + CH_3Cl$ collisions studied above, i.e., 126.4

(46) The initial energy for these trajectories is partitioned with the fractions 0.00, 0.21, and 0.79 in rotation, vibration, and relative translation, respectively. The average values for these fractions in the products are respectively 0.09, 0.33, and 0.58. Thus, the CH_3 rocking excitation is transferred to CH_3Cl product vibration. The increase in CH_3Cl vibrational energy in going from reactants to products is similar to that seen without CH_3 rocking excitation (see Table 1).

Table 2. D_{3h} and C_s Barrier Properties and CPU Time for Direct Dynamics at Different Levels of Electronic Structure Theory[a]

theory	D_{3h} barrier			C_s barrier			relative CPU time
	energy[b]	C−Cl	C−H	energy[c]	C−Cl	Cl−C−Cl	
HF/3-21+G*	2.06	2.40	1.06	54.70	2.70	92.8	1.00
HF/6-31G*	3.57	2.38	1.06	56.34	2.73	95.2	1.14
HF/6-31G**	3.42	2.38	1.06	55.30	2.75	96.8	1.49
HF/6-31+G*	6.59	2.39	1.06	57.78	2.79	98.6	1.59
HF/6-311++G**	6.91	2.39	1.06	56.78	2.81	101.2	8.52
MP2/6-31G*	4.54	2.31	1.07	55.56	2.42	85.1	3.05
MP2/6-31G**	4.52	2.30	1.07	55.04	2.41	85.4	4.24
MP2/6-31+G*	7.66	2.32	1.07	56.68	2.44	84.2	4.58
MP2/6-311++G**	7.96	2.30	1.07	56.01	2.40	84.7	23.14
CCSD(T)/367cGTOs	3.16	2.31	1.07				

[a] Energies are in kcal/mol, distances in Å, and angles in deg. The relative direct dynamics CPU time is for calculations using one processor on a SGI/MIPS R10000 workstation. [b] The classical potential energy barrier. Including harmonic zero-point energies lowers the barrier by 0.3−0.5 kcal/mol. [c] The classical potential energy barrier. Including harmonic zero-point energies lowers the barrier by ∼1−2 kcal/mol.

kcal/mol. Zero-point energy was added to the barrier's normal modes of vibration and $RT/2$, with $T = 300$ K, was added to each of the barrier's principal rotation axis. These zero-point and rotational energies are 23.6 and 0.9 kcal/mol, respectively, and the barrier's potential energy is 54.7 kcal/mol. Thus, to attain the desired total energy, 47.2 kcal/mol was added to reaction coordinate translation. Random initial conditions for these trajectories arise from random phases for the normal mode vibrations, and a random sign (i.e. positive or negative) for each component of the rotational angular momentum and for the reaction coordinate momentum. With CH_3Cl zpe removed, the average product energy partitioning for these trajectories is very specific, i.e., $f_{rel} = 0.11$, $f_{vib} = 0.83$, and $f_{rot} = 0.06$, and is primarily to product vibration.[47] This is distinctly different from the results in Table 1 for translational activation of reaction 1, which occurs by backside attack and for which only ∼10% of the available energy goes to product vibration. The strong implication is that the C_s barrier structure cannot be attained by translational activation and, instead, requires preferential vibrational excitation of CH_3Cl.

MP2/6-31G* direct dynamics was also used to study energy partitioning for the trajectories initiated at the C_s barrier (properties of the D_{3h} and C_s barriers at this level of theory are given in Table 2). A total of 29 MP2 trajectories were calculated and the product energy partitioning obtained is $f_{rel} = 0.23$, $f_{vib} = 0.63$, and $f_{rot} = 0.14$. As found from the HF/3-21+G* trajectories, the energy partitioning is preferentially directed to product vibration.

Summary

The work reported here illustrates the power of ab initio direct dynamics simulations for probing microscopic reaction mechanisms and calculating experimental observables. With direct dynamics, the classical dynamics of an ab initio level of theory is not adulterated by a less than exact fitting with an analytic potential energy function. For the 100 kcal/mol translational activation of reaction 1, the HF/3-21+G* level of theory predicts a backside reaction mechanism with a reaction cross section only 2−4 times larger than the experimental value.[4] The product energy partitioning, velocity scattering angle distributions, and angular momentum correlations from the HF/3-21+G* direct dynamics trajectories are very similar to results from a previous classical trajectory study[23] based on the PES3 analytic potential energy surface. The principal difference in these two trajectory studies is the approximately 10 times smaller reaction cross section for the HF/3-21+G* trajectories.

Reaction by a frontside displacement mechanism is not observed in the $Cl^- + CH_3Cl$ direct dynamics trajectories. Initializing trajectories at the frontside C_s barrier and propagating them to products preferentially puts more than 80% of the available energy in product vibration. This suggests that translational activation cannot access the frontside barrier and, instead, extensive CH_3Cl vibrational excitation may be needed. However, C−Cl stretch excitation promotes the backside pathway[6,12,17,28] and it is possible, even with vibrational excitation, that the frontside pathway will be overwhelmed by backside reaction.

It would be of interest to investigate the direct dynamics of reaction 1, with both vibrational and translational activation, at a higher level of ab initio theory. A comparison of barrier heights and structures and the CPU time requirement for direct dynamics at different levels of electronic structure theory are given in Table 2. For example, the MP2/6-31G* level of theory gives classical barriers of 4.5 and 55.6 kcal/mol for the backside D_{3h} and frontside C_s barriers, in approximate agreement with the G2(+)[20,21] and CCSD(T)[24] barriers. The barrier structures at this MP2 level are in excellent agreement with the higher level structures.[20,21,24] For example, MP2/6-31G* has a D_{3h} barrier with C−Cl and C−H bond lengths of 2.31 and 1.07 Å, in exact agreement with the CCSD(T) result.[24] Similarly, the MP2/6-31G* C_s barrier has a C−Cl bond length and Cl−C−Cl angle of 2.42 Å and 85.1°, which are in very good agreement with the MP2/6-311++G** structure. Though a MP2/6-31G* direct dynamics trajectory will require approximately 3 times more computer time than the HF/3-21+G* trajectories reported here, a MP2 direct dynamics study is feasible with parallel and distributed computer architectures.

For the concerted backside and frontside pathways for reaction 1 the HF/3-21+G* level of theory gives transition state structures and energies in good agreement with those of higher levels of theory. Thus, HF/3-21+G* direct dynamics is a realistic approach for investigating the translational activation of reaction 1. However, HF theory does not properly describe bond ruptures [48] and could not be used to study the C−Cl bond dissociation pathway of vibrationally excited CH_3Cl.[49] Translational activation of reaction 1 does not produce vibrationally excited CH_3Cl. As shown in Table 1, with a high reagent

(47) For the 24 HF/3-21+G* trajectories initiated at the C_s transition state the average and range of the $\theta(l_f,j_f)$, $\theta(l_f,J)$, and $\theta(j_f,J)$ angular momentum scattering angles in degrees are 123 (76−150), 51 (11−104), and 72 (25−134), respectively. The average and range of values in $\hbar$ for the l_f, j_f, and J angular momenta are 67 (28−121), 57 (20−107), and 63 (52−74), respectively.

(48) Levine, I. N. *Quantum Chemistry*, 3rd ed.; Allyn and Bacon: Boston, 1983; p 380.

(49) The classical CH_3−Cl bond energy is 49.9 and 81.8 kcal/mol at the HF/3-21+G* and MP2/6-31G* levels of theory, respectively. The experimental value for this bond energy is 87.4 kcal/mol.[10]

translational energy of 100 kcal/mol, the average vibrational energy in the CH_3Cl product is 10 kcal/mol, with a maximum value of 29 kcal/mol. On the other hand, some of the trajectories initiated at the C_s barrier form vibrationally excited CH_3Cl with sufficient energy to dissociate to $CH_3 + Cl$ and/or $CH_2 + HCl$.[50] However, these trajectories were only followed as they moved off the C_s barrier and they were not integrated for longer times to study CH_3Cl dissociation. As discussed above, HF theory is clearly inappropriate for the C−Cl bond rupture channel and a higher level of theory is needed to properly describe both the HCl elimination and C−Cl unimolecular rupture pathways. Because of the rather lengthy times often required for energy to accumulate in the reaction coordinate for a unimolecular reaction to occur, direct dynamics may be prohibitively expensive for studying CH_3Cl dissociation. In conclusion, it is apparent that considerable care is required in applying HF direct dynamics.

(50) The 0 K energy difference between $^1CH_2 + HCl$ and CH_3Cl is 97.8 kcal/mol: Lide, D. R. *CRC Handbook of Chemistry and Physics*, 79th ed.; CRC Press: New York, 1998. HF/3-21+G* and MP2/6-31G* give 88.4 and 111.2 kcal/mol for this energy difference, respectively.

Acknowledgment. This research was supported by the National Science Foundation. The authors wish to thank Professor H. Bernhard Schlegel for helpful discussions concerning the interface between VENUS96 and Gaussian, and David J. Mann for helpful discussions concerning the reaction dynamics on PES3.

JA990607J